J. Geogr. Sci. 2010, 20(3): 323-332
DOI: 10.1007/s11442-010-0323-6

Spatial and temporal variation of global LAI during 1981–2006

LIU Siliang[1,2], *LIU Ronggao[1], LIU Yang[1,2]

1. Institute of Geographic Sciences and Natural Resources Research, CAS, Beijing 100101, China
2. Graduate University of Chinese Academy of Sciences, Beijing 100049, China

Abstract: Earth is always changing. Knowledge about where changes happened is the first step for us to understand how these changes affect our lives. In this paper, we use a long-term leaf area index data (LAI) to identify where changes happened and where has experienced the strongest change around the globe during 1981–2006. Results show that, over the past 26 years, LAI has generally increased at a rate of 0.0013 per year around the globe. The strongest increasing trend is around 0.0032 per year in the middle and northern high latitudes (north of 30°N). LAI has prominently increased in Europe, Siberia, Indian Peninsula, America and south Canada, South region of Sahara, southwest corner of Australia and Kgalagadi Basin; while noticeably decreased in Southeast Asia, southeastern China, central Africa, central and southern South America and arctic areas in North America.

Keywords: global change; leaf area index; spatiotemporal variation; hot-spot areas

1 Introduction

Earth is always changing. However, many evidences have shown that recent human actions accelerated these changes and some changes may be irreversible (IPCC, 2007). These changes would seriously affect our lives so that they are concerned by people from various disciplines. Knowledge about where changes happened is the first step to understand what has led to these changes and what steps should be taken to control them. Vegetation covers three-fourths of the Earth's land surface, and plays a key role in global hydrological, biochemical cycles and energy balance. In the context of global change, vegetation has changed as it responds to rising temperature, shifting precipitation patterns and other factors (IPCC, 2007). This vegetation change would alter global matter and energy cycle, and has feedback effects to climate. Owing to uneven distribution of natural and anthropogenic impacts and differential response of different vegetation types, the spatial distribution of the change is stratified. Where changes happened? Which place has experienced the most dramatic change? And what kind of change has occurred? The answers to these problems are important for

Received: 2009-08-07 **Accepted:** 2009-12-18
Foundation: 863 Program, No.2007AA12Z158; National Science & Technology Pillar Program, No.2006BAC08B04; 2008BAK50B06; 2008BAK49B01
Author: Liu Siliang (1986–), MA Candidate, specialized in quantitative remote sensing. E-mail: lslrsgis@gmail.com
***Corresponding author:** Liu Ronggao, E-mail: liurg@igsnrr.ac.cn

global environmental research.

Satellite remote sensing serves as the most effective means to track the changes of earth with its distinct advantage in collecting global data with every day since the 1970s. AVHRR Normalized Difference Vegetation Index (NDVI) series were employed as the proxy to study long term variation of vegetation at global or continental scale. Plant growth in the northern high latitudes was found increased during 1981–1991 from GIMMS NDVI and PAL NDVI data sets (Myneni *et al*., 1997; Myneni *et al*., 1998). The subsequent work confirmed this finding using NDVI from 1981–1999 (Lucht *et al*., 2002; Slayback *et al*., 2003), and suggested that temperature rising is probably the primary cause for vigorous vegetation growth in the northern high latitudes (Zhou *et al*., 2003; Zhou *et al*., 2001). Later, Xiao and Moody (2005) correlated global vegetation activities with climate using NDVI from 1981–1998, and identified regions highly controlled by temperature and precipitation. All these studies employed NDVI as the indicator of vegetation growth status. However, different sensors have distinct spectral responses which affect NDVI value (Trishchenko *et al*., 2002). And significant artificial anomalies within NDVI were found owing to orbit drift and illumination effects (Cuomo *et al*., 2001; Sobrino *et al*., 2008). In addition, these studies only analyzed the data before 2000.

LAI, defined as half the total leaf area per unit ground (Chen and Black, 1992), is directly linked to vegetation activities and comparable among different ecosystems. It has removed the effects of spectral response, illumination and orbit drift during data acquisition. It should be better, at least theoretically, than NDVI as the indicator of vegetation status. The objective of this paper is to use LAI to estimate global vegetation variation trend and identify hot-spot areas of this change during 1981–2006. First, temporal variation of global leaf area in this period is presented. Then, geographic distribution of global LAI trend over the 26 years is mapped, and the hot-spot areas with extreme trends are identified.

2 Method

A 26-year LAI data record is generated by a retrieval algorithm based on 4-Scale model, at 8 km resolution and a bimonthly (half a month) time step, from July 1981 to December 2006. The spatial extent is 63°S–90°N, 180°W–180°E. All continents except Antarctic are included in the data record. The algorithm uses GIMMS NDVI (Tucker *et al*., 2005) and UMD land cover (Hansen *et al*., 2000) as input. Specific description of the algorithm is given by Deng *et al*. (2006) and Liu *et al*. (2007).

Let $LAI(Y, HM, L, C)$ be LAI of pixel at line L, column C, in bimonth HM, and year Y. The average annual LAI is calculated as

$$\overline{LAI}(HM, L, C) = \frac{1}{N_y} \sum_{Y=1982}^{2006} LAI(Y, HM, L, C) \tag{1}$$

where N_y is the number of years ($N_y = 25$). The anomaly of LAI is defined as

$$LAI\_Anomaly(Y, HM, L, C) = LAI(Y, HM, L, C) - \overline{LAI}(HM, L, C) \tag{2}$$

The average LAI of a certain latitudinal zone is calculated as

$$\overline{LAI}(HM) = \frac{1}{N_y} \frac{1}{N_{LS}} \frac{1}{N_c} \sum_{Y=1982}^{2006} \sum_{L=L_1}^{L_2} \sum_{C} LAI(Y, HM, L, C) \tag{3}$$

where L_1 and L_2 are the start line and end line of a certain latitudinal band, respectively, N_{LS} is the number of selected lines ($N_{LS} = L_2 – L_1 + 1$) and N_c is the number of columns. If $N_{LS} = N_L$ (total number of lines), then $\overline{LAI}(HM)$ is the global average LAI. And the average LAI anomaly of a certain latitudinal band is calculated as

$$\overline{LAI\_Anomaly}(HM) = \frac{1}{N_y}\frac{1}{N_{LS}}\frac{1}{N_c}\sum_{Y=1982}^{2006}\sum_{L=L_1}^{L_2}\sum_{C} LAI\_Anomaly(Y, HM, L, C) \quad (4)$$

Global and regional mean LAI is obtained by averaging all pixels with non-zero leaf area index in an equal-area Sinusoidal projection.

3 Results

3.1 Temporal variation of LAI

The whole imagery coverage is divided into six latitudinal bands, 50°–90°N, 30°–50°N, 10°–30°N, 10°S–10°N, 10°–30°S and 63°–30°S, to analyze the different temporal distribution in distinct latitudes. Figure 1 presents the time series of spatially averaged LAI in global coverage and six latitudinal bands, which are obtained by averaging non-zero LAI in corresponding extents. The winter time LAI at latitudes north of 50°N is close to zero, mainly due

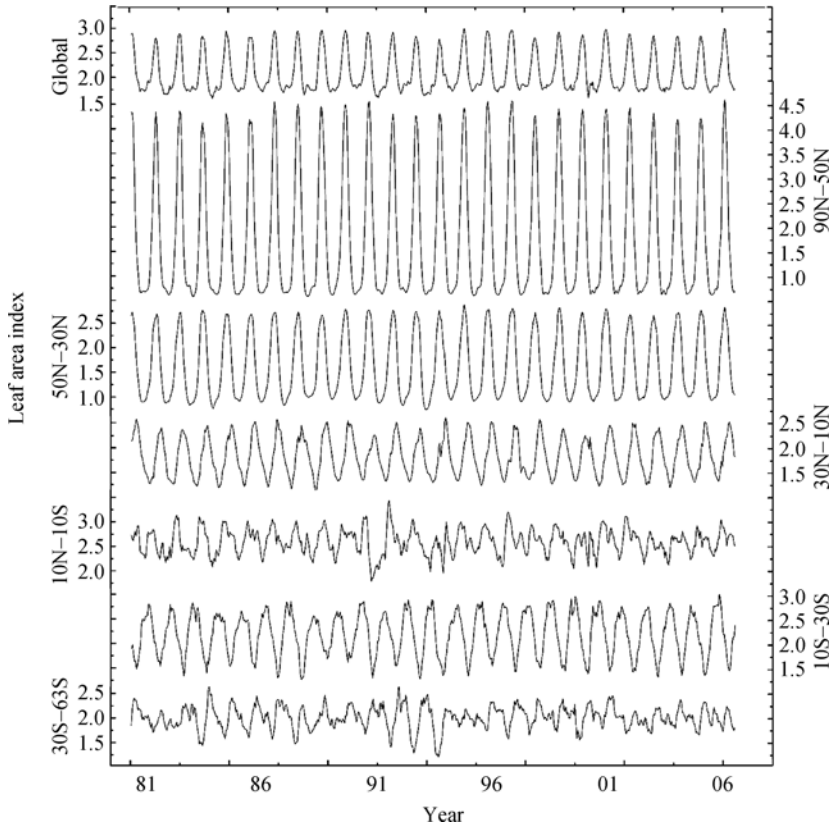

Figure 1 Spatially averaged LAI time series in global coverage and six latitudinal bands from July 1981 to December 2006

to lack of valid winter time data. As expected, the LAI in the Southern Hemisphere shows the opposite seasonality. Notable annual cycle can be observed in global coverage and all latitudinal bands except 10°S–10°N and 63°–30°S (Figure 1). The magnitude sequence of LAI range is: 50°–90°N (0.5–4.5), 30°–50°N (1.0–2.5), 10°–30°S (1.5–3.0), 0°–30°N (1.5–2.5), 10°S–10°N (2.0–3.0) and 63°–30°S (1.5–2.5). This result suggests that LAI range is wider in the Northern Hemisphere than the equatorial zone and the Southern Hemisphere.

LAI anomaly is calculated by subtracting LAI mean values from corresponding original LAI values in each bimonth. In global coverage and each latitudinal band, it shows positive trend over the past 26 years. In global coverage, LAI has been increasing at a rate of 0.0013 per year during July 1981–December 2006 (Figure 2). In the middle and northern high latitudes (30°–50°N and 50°–90°N), LAI exhibits the strongest increasing trend, around 0.0032 per year. This is consistent with persistent greening in northern high-latitudes reported by (Myneni *et al*., 1997). The magnitude sequence of the increasing trend is: 50°–90°N > 30°–50°N > 63°–30°S > 10°–30°N > 30°–10°S > 10°S–10°N (Figure 2).

The effect of inter-calibration can be observed in LAI anomaly time series. The most prominent period is from September 1994 until January 1995. During this period, data from

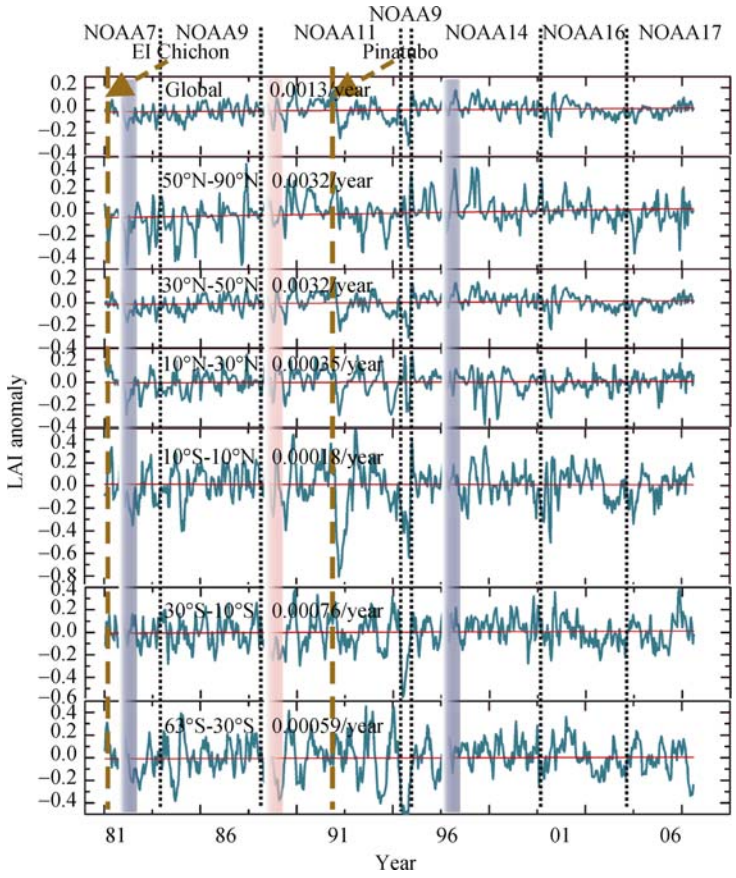

Figure 2 LAI anomaly time series in global region and a series of latitudinal bands. Linear trend of LAI anomaly is plotted in red straight line. El Niño events and La Niña events are symbolized by blue and red gradually changed vertical bars, respectively, where saturation represents the magnitude and width shows the temporal range. Mt. El Chichon and Mt. Pinatubo eruptions are marked by brown vertical dash lines. Red straight line indicates the linear trend

NOAA9 was used when NOAA11 started to malfunction and its replacement, NOAA13, failed shortly after launch. When shifting from NOAA11 to NOAA9 in September 1994, LAI anomaly increases sharply (Figure 2). This indicates that the inter-calibration has significant effects in this period.

Shortly after the eruption of Mt. El Chichon in April 1982 and Mt. Pinatubo in June 1991, LAI anomaly falls down steeply, which can be observed in global coverage and each latitudinal band (Figure 2). This abrupt decline is most prominent in equatorial zone (10°S–10°N), and less prominent in the high latitudes (50°–90°N, 63°–30°S). In addition, it sustained in the low level for more than one year, which is consistent with the lifespan of troposphere aerosol caused by volcanic eruption. Moreover, the decrease of LAI anomaly is much more prominent after Mt. Pinatubo eruption than after Mt. El Chichon, which is consistent with the fact that the cooling effect of the former was stronger than the latter, injecting double amount of SO_2 into the atmosphere than the latter (Self and Mouginismark, 1995).

3.2 Spatial distribution of LAI trend

Spatial distribution of linear trend in estimated LAI from 1982–2006 is shown in Figure 3a. Spatially averaged LAI is mapped in Figure 3b for comparison. The LAI linear trend is regressed against time at the original 8 km pixel scale. Due to the abrupt decline of LAI anomaly after Mt. Pinatubo eruption, the one and a half year after the Mt. Pinatubo eruption are masked in regression analysis. Only regions with linear trend of possibility greater than 95% are mapped. Cell grids showing positive or negative LAI trends are not randomly interspersed across the continent, but aggregated displaying clear spatial patterns. In most regions, LAI has increased (Figure 3a).

The hot-spot areas of LAI change can also be observed. In Europe, Siberia, northeastern China, eastern and central America, Indian Peninsula, south edge of Sahara, Kgalagadi Basin, southwestern corner of Australia and regions along the Gulf of Carpentaria, LAI shows increasing trend. In central Canada, west Canada, Alaska, Southeast Asia, southeastern China, central Africa, central and eastern Argentina, LAI is decreasing (Figure 3a).

3.2.1 Regions with positive LAI trend

In these hot-spot areas, different LAI trend can be observed. In Europe, Siberia, and northeastern China, LAI exhibits positive trend. Interestingly, these areas with high LAI trend correspond to those with high LAI value (Figure 3b). The growth of the vegetation in these middle and high latitude areas is mainly limited by temperature. Many studies correlating NDVI with land surface temperature indicate warming might be the most important factor accounting for the LAI increase in this area (Myneni *et al*., 1997; Slayback *et al*., 2003; Zhou *et al*., 2001). Warming, causes longer active growing season length and higher growth magnitude, therefore leads to increase in LAI in this area (Myneni *et al*., 1997).

In eastern and central America, LAI shows positive trend. The primary cause is similar as in Europe, Siberia and northeastern China. Warming, causes longer active growing season length and higher growth magnitude, therefore leads to increase in LAI in this area.

In Indian Peninsula, LAI shows increasing trend across the entire peninsula. The preliminary results indicate that positive trends in vegetation change occurred over most parts of the country and these changes appear not to be highly correlated with rainfall data, indicating that land cover transformations may be the major driving force behind the changes

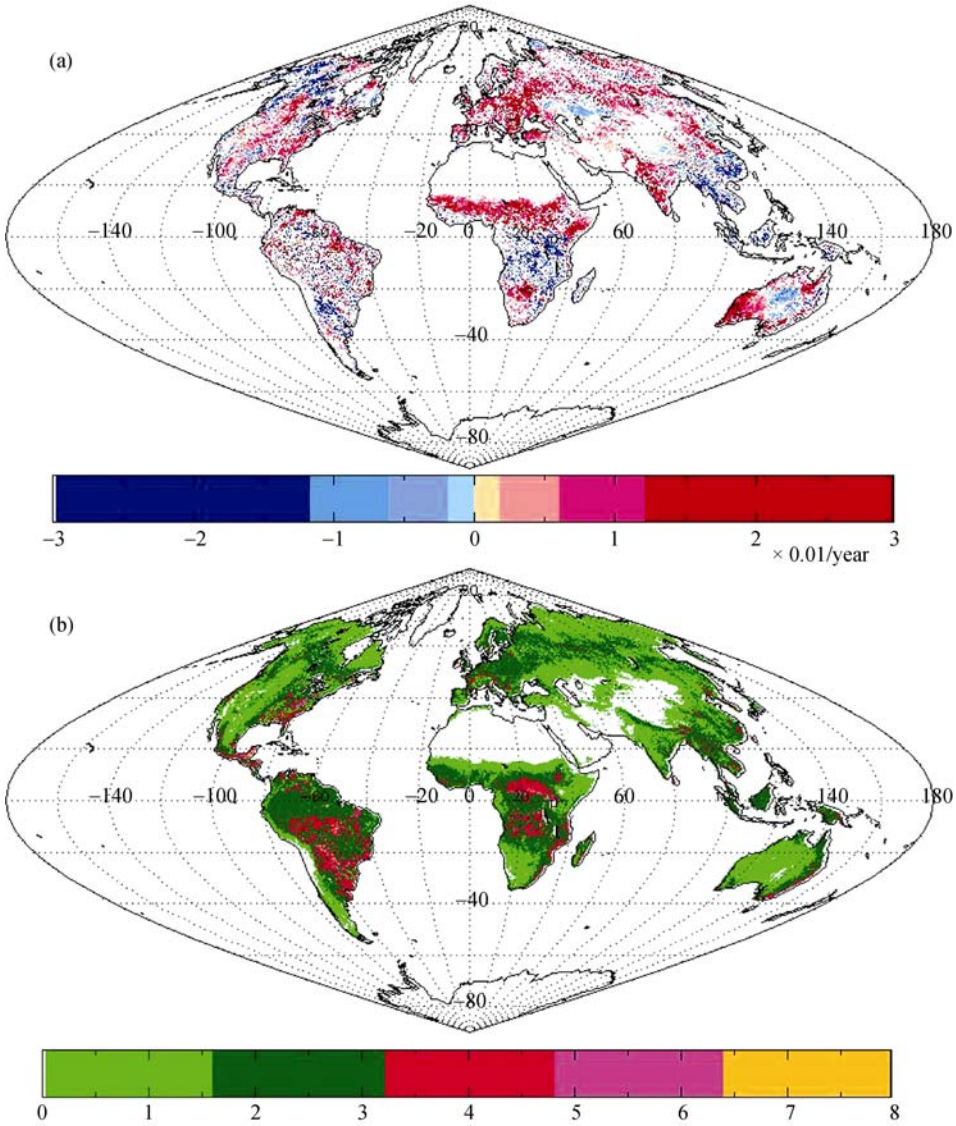

Figure 3 (a) Geographic distribution of spatial averaged LAI. This spatial averaged LAI is calculated by averaging LAI value in all bimonths from 1982–2006. (b) Spatial distribution of linear trends in estimated LAI from July 1981–December 2006. Due to the abrupt decline of LAI anomaly after Mt. Pinatubo eruption, the one and a half year after the Mt. Pinatubo eruption (July 1991–December 1992) are masked in regression analysis

(Jeyaseelan *et al*., 2007).

Along the band south to Sahara extending from Guinea to Ethopia, LAI shows high increasing trend. This is a transitional belt from semi-desert (north) to grassland (central) to savanna (south). The climate of this region is characterized by a marked seasonality with a long dry season and a short humid season, thus vegetation growth is highly limited by the available water. Rainfall emerges as the dominant causative factor in the dynamics of vegetation greenness in the Sahel at an 8 km spatial resolution, and human impact might be another factor (Herrmann *et al*., 2005).

In Kgalagadi Basin, LAI shows prominent positive trend. Red dune and scrub are the

dominant land cover types there. Vegetation growth in this semi-arid area is highly controlled by precipitation. One month lagged correlation analysis suggests that substantial increase in vegetation is primarily due to increased rainfall (Funk and Brown, 2006).

In southwestern corner of Australia and regions along the Gulf of Carpentaria, LAI shows significant increasing trend. The southwestern corner is a winter cereal-cropping zone with forest cover along the coastal hinterland. Along the Gulf of Carpentaria, treeless grasslands support extensive pastoralism. Substantial rainfall increase was observed over the 26 years in these two areas. Correlation analysis suggests that rainfall increase is probably the primary factor for LAI increase in these two areas (Donohue *et al*., 2009).

3.2.2 Regions with negative LAI trend

In central Canada, west Canada and Alaska, LAI shows negative trend. The result in Canada is a little different from that obtained by Pouliot *et al*. (2009), who found that vegetation increased in most parts of Canada using NDVI from 1985–2006. This discrepancy might be caused by different temporal span and distinct treatment of original NDVI data. The results in Alaska are consistent with previous studies. The summer warming in arctic Alaska may be due to a lengthening of the snow-free season, with early sensible heating of the lower atmosphere (Chapin *et al*., 2005). Recent study shows that decrease in interior Alaska is mainly the consequence of fire (Goetz *et al*., 2005).

In Southeast Asia, the clearance for agriculture and timber production is prevalent in most countries of this region. Fires to clear forest and brush have been an annual occurrence in this region for generations. Especially the widespread series of fires, which occurred mainly in Indonesia between April and November of 1997, destroyed large amount of rainforest (Sastry, 2002).

In southeastern China, LAI shows negative trend. During 1981–1993, China started a series of major ecological projects aimed at environmental protection with forests, and forest cover increased 1.26 percentage points from afforestation (Zhang and Song, 2006). During 1993–2003, forest plantation are reported more rapid than in 1981–1993 in China (Zhang and Song, 2006). However, LAI shows negative trend. This might be caused by intensive human activities, especially land use change caused by built-up area expansion accompanying urbanization. These effects are postulated to overweight the effects of afforestation.

In central Africa (excluding Congo Basin), LAI decreased prominently during 1981 to 2006. This decrease may be due to precipitation and deforestation. The dominant vegetation type here is savanna and scrub. The growth of the vegetation is highly controlled by rainfall. One month lagged correlation analysis suggests that substantial increase in vegetation might be primarily due to increased rainfall (Funk and Brown, 2006).

In central and eastern Argentina, LAI shows pronounced negative trend. In the western part of this region, the dominant vegetation type is dry tropical forests. LAI is fairly high in this area, about 3–5 (Figure 3b). Land use change might be the leading factors contributing LAI decrease. The conversion form forests to pasture would lead to decrease in NDVI (Paruelo *et al*., 2004), hence decrease in retrieved LAI. In central and eastern part of this region, the dominant vegetation type is pampas. The primary limitation of plant growth there is precipitation. It is postulated that precipitation change might be the most important factor leading to vegetation decrease in this area.

3.2.3 Amazon Basin and Congo Basin

Besides these hot-spot areas, Amazon Basin and Congo Basin are also the foci of vegeta-

tion change studies. The variation of leaf area there is important for global vegetation research, since they are the two largest rainforests around the globe. In interior Amazon Basin, LAI shows a negative trend from July 1981–December 2006. The pattern of LAI trend is spurious, the decrease in most areas is not prominent and the most decrease concentrated in the northwestern Amazon. The decrease of leaf area is mainly due to continuous deforestation, which is consistent with previous studies. By 2001, about 837,000 km^2 of Amazonian forests had been cleared (Soares *et al*., 2006), with 1990s gross rates of ~25,000 km^2 $year^{-1}$ (Achard *et al*., 2002).

In Congo Basin, LAI is also decreasing, but the decrease is much less prominent than in Amazon. This is mainly due to deforestation and forest degradation. Although deforestation is a severe problem in some parts, to whole Congo Basin, it is less severe as in Amazon Basin. A recent analysis estimates that Africa accounted for less than 6% of the total loss of humid forest cover during the 1990s, whereas Brazil's loss represented nearly half of the total (Koenig, 2008).

4 Discussion

Degradation of NDVI over time and NDVI's shifts between the satellites would detriment the accuracy of retrieved LAI, and thus the linear trend obtained from analysis of long-term LAI. GIMMS uses preflight calibration to relate Channel 1 and Channel 2 reflectance to a preflight calibration standard on the ground. However, this preflight calibration does not take sensor degradation into consideration (Los, 1998). In addition, NDVI's shifts between the satellites caused by differential sensor-intrinsic characteristics are not addressed in producing GIMMS NDVI.

LAI is found falling down abruptly after Mt. Pinatubo eruption. This finding is consistent with reports from Buermann *et al*. (2002) and Lucht *et al*. (2002), which may be due to incomplete aerosol correction and aerosol cooling effects. Although the negative effects of stratosphere aerosol on GIMMS NDVI have been corrected, this correction is not completed (Zhou *et al*., 2001). In addition, the cooling effects also contribute to the abrupt decrease. Previous studies suggest that stratosphere aerosol would slow down the growth of vegetation in middle and high latitudes, although it would enhance growth in tropical areas (Gu *et al*., 2003).

El Niño-Southern Oscillation (ENSO), the global coupled ocean-atmosphere phenomenon, has direct and indirect impact on vegetation growth. Strong ENSO events have consequences on vegetation growth in tropical areas mainly through affecting the rainfall pattern. In addition, ENSO is associated with floods, droughts, and other disturbances in a range of locations around the world. These disturbances would impact vegetation growth in regional scale. ENSO can be divided into two phases: El Niño (warm events) and La Niña (cold events). These two phases exert substantial different impacts on vegetation around the globe, especially in the Pacific coastal areas (Buermann *et al*., 2002). There are three strong ENSO events during July 1981–December 2006, which are: El Niño event in 1982–1983, La Niña event in 1988–1989, and El Niño event in 1997–1998 (Figure 3b). The effects of these strong ENSO events are not negligible in analyzing LAI trend during 1981–2006.

To better estimate LAI trend, degradation of NDVI over time and NDVI's shifts between the satellites should be taken into consideration. In addition, stratosphere aerosol effects

should be removed from apparent NDVI signals. In attempt to further investigate the causes for leave area change, climate factors, disturbances and anthropogenic activities should be taken into consideration. Correlation analysis has shown the ability to uncover the mechanism of ecosystem response to some extent (Xiao and Moody, 2005; Zhou *et al*., 2003). Future studies should focus on exploring the causes for LAI variation in these hot-spot areas.

5 Conclusions

(1) Annual cycle is prominent in global coverage and all six latitudinal bands except 10°S–10°N and 63°–30°S. Comparatively, seasonal variation of average LAI and accumulated LAI in the Northern Hemisphere is pronounced while the one in the Southern Hemisphere and tropical bands is near stationary.

(2) Shortly after the eruption of Mt. El Chichon in April 1982 and Mt. Pinatubo in June 1991, LAI anomaly falls down abruptly, which can be observed in global coverage and each latitudinal band. This abrupt decline is most prominent in the equatorial zone (10°S–10°N), and less prominent in the high latitudes (50°–90°N, 63°–30°S).

(3) In global coverage, LAI has increased at a rate of 0.0013 per year during July 1981–December 2006. All latitude bands show positive trend, and the one in 50°–90°N, 30°–50°N is the highest (0.0032/year). The linear trend in LAI is significantly positive in Europe, Siberia, northeastern China, eastern and central America, Indian Peninsula, south edge of Sahara, Kgalagadi Basin, southwestern corner of Australia and regions along the Gulf of Carpentaria, and negative in central Canada, west Canada, Alaska, Southeast Asia, southeastern China, central Africa, and central and eastern Argentina.

Acknowledgement

The authors thank Chen J M (University of Toronto) for providing the 4-Scale model. This work is part of the 863 Program and National Science & Technology Pillar Program.

References

Achard F, Eva H D, Stibig H J *et al*., 2002. Determination of deforestation rates of the world's humid tropical forests. *Science*, 297(5583): 999–1002.

Buermann W, Wang Y J, Dong J R *et al*., 2002. Analysis of a multiyear global vegetation leaf area index data set. *Journal of Geophysical Research-Atmospheres*, 107(D22): 4646.

Chen J M, Black T A, 1992. Defining leaf area index for non-flat leaves. *Plant Cell and Environment*, 15(4): 421–429.

Cuomo V, Lanfredi M, Lasaponara R *et al*., 2001. Detection of interannual variation of vegetation in middle and southern Italy during 1985–1999 with 1 km NOAA AVHRR NDVI data. *Journal of Geophysical Research-Atmospheres,* 106(D16): 17863–17876.

Deng F, Chen J M, Plummer S *et al*., 2006. Algorithm for global leaf area index retrieval using satellite imagery. *IEEE Transactions on Geoscience and Remote Sensing*, 44(8): 2219–2229.

Donohue R J, McVicar T R, Roderick M L, 2009. Climate-related trends in Australian vegetation cover as inferred from satellite observations, 1981–2006. *Global Change Biology*, 15(4): 1025–1039.

Funk C C, Brown M E, 2006. Intra-seasonal NDVI change projections in semi-arid Africa. *Remote Sensing of Environment*, 101(2): 249–256.

Goetz S J, Bunn A G, Fiske G J *et al*., 2005. Satellite-observed photosynthetic trends across boreal North America

associated with climate and fire disturbance. *Proceedings of the National Academy of Sciences of the United States of America*, 102(38): 13521–13525.

Gu L H, Baldocchi D D, Wofsy S C *et al*., 2003. Response of a deciduous forest to the Mount Pinatubo eruption: Enhanced photosynthesis. *Science*, 299(5615): 2035–2038.

Hansen M C, Defries R S, Townshend J R G *et al*., 2000. Global land cover classification at 1km spatial resolution using a classification tree approach. *International Journal of Remote Sensing*, 21(6/7): 1331–1364.

Herrmann S M, Anyamba A, Tucker C J, 2005. Recent trends in vegetation dynamics in the African Sahel and their relationship to climate. *Global Environmental Change-Human and Policy Dimensions*, 15(4): 394–404.

Jeyaseelan A T, Roy P S, Young S S, 2007. Persistent changes in NDVI between 1982 and 2003 over India using AVHRR GIMMS (global inventory Modeling and mapping studies) data. *International Journal of Remote Sensing*, 28(21): 4927–4946.

Koenig R, 2008. Critical time for African rainforests. *Science*, 320(5882): 1439–1441.

Liu R, Chen J M, Liu J *et al*., 2007. Application of a new leaf area index algorithm to China's landmass using MODIS data for carbon cycle research. *Journal of Environmental Management*, 85(3): 649–658.

Los S O, 1998. Estimation of the ratio of sensor degradation between NOAA AVHRR channels 1 and 2 from monthly NDVI composites. *IEEE Transactions on Geoscience and Remote Sensing*, 36(1): 206–213.

Lucht W, Prentice I C, Myneni R B, 2002. Climatic control of the high-latitude vegetation greening trend and Pinatubo effect. *Science*, 296(5573): 1687–1689.

Myneni R B, Keeling C D, Tucker C J, 1997. Increased plant growth in the northern high latitudes from 1981 to 1991. *Nature*, 386(6626): 698–702.

Myneni R B, Tucker C J, Asrar G *et al*., 1998. Interannual variations in satellite-sensed vegetation index data from 1981 to 1991. *Journal of Geophysical Research-Atmospheres*, 103(D6): 6145–6160.

Paruelo J M, Garbulsky M F, Guerschman J P *et al*., 2004. Two decades of Normalized Difference Vegetation Index changes in South America: Identifying the imprint of global change. *International Journal of Remote Sensing*, 25(14): 2793–2806.

Pouliot D, Latifovic R, Olthof I, 2009. Trends in vegetation NDVI from 1 km AVHRR data over Canada for the period 1985–2006. *International Journal of Remote Sensing*, 30(1): 149–168.

Sastry N, 2002. Forest fires, air pollution, and mortality in Southeast Asia. *Demography*, 39(1): 1–23.

Self S, Mouginismark P J, 1995. Volcanic eruptions, predictions, hazard assessment, remote sensing, and social implications. *Reviews of Geophysics,* 33: 257–262.

Slayback D A, Pinzon J E, Los S O *et al*., 2003. Northern hemisphere photosynthetic trends 1982–99. *Global Change Biology*, 9(1): 1–15.

Soares B S, Nepstad D C, Curran L M *et al*., 2006. Modelling conservation in the Amazon basin. *Nature*, 440(7083): 520–523.

Sobrino J A, Julien Y, Atitar M *et al*., 2008. NOAA-AVHRR orbital drift correction from solar zenithal angle data. *IEEE Transactions on Geoscience and Remote Sensing*, 46(12): 4014–4019.

Trishchenko A P, Cihlar J, Li Z Q, 2002. Effects of spectral response function on surface reflectance and NDVI measured with moderate resolution satellite sensors. *Remote Sensing of Environment*, 81(1): 1–18.

Tucker C J, Pinzon J E, Brown M E *et al*., 2005. An extended AVHRR 8-km NDVI dataset compatible with MODIS and SPOT vegetation NDVI data. *International Journal of Remote Sensing*, 26(20): 4485–4498.

Xiao J, Moody A, 2005. Geographical distribution of global greening trends and their climatic correlates: 1982–1998. *International Journal of Remote Sensing*, 26(11): 2371–2390.

Zhang Y X, Song C H, 2006. Impacts of afforestation, deforestation, and reforestation on forest cover in China from 1949 to 2003. *Journal of Forestry*, 104(7): 383–387.

Zhou L, Kaufmann R K, Tian Y *et al*., 2003. Relation between interannual variations in satellite measures of northern forest greenness and climate between 1982 and 1999. *Journal of Geophysical Research-Atmospheres*, 108(D1): 4004.

Zhou L M, Tucker C J, Kaufmann R K *et al*., 2001. Variations in northern vegetation activity inferred from satellite data of vegetation index during 1981 to 1999. *Journal of Geophysical Research-Atmospheres*, 106(D17): 20069–20083.